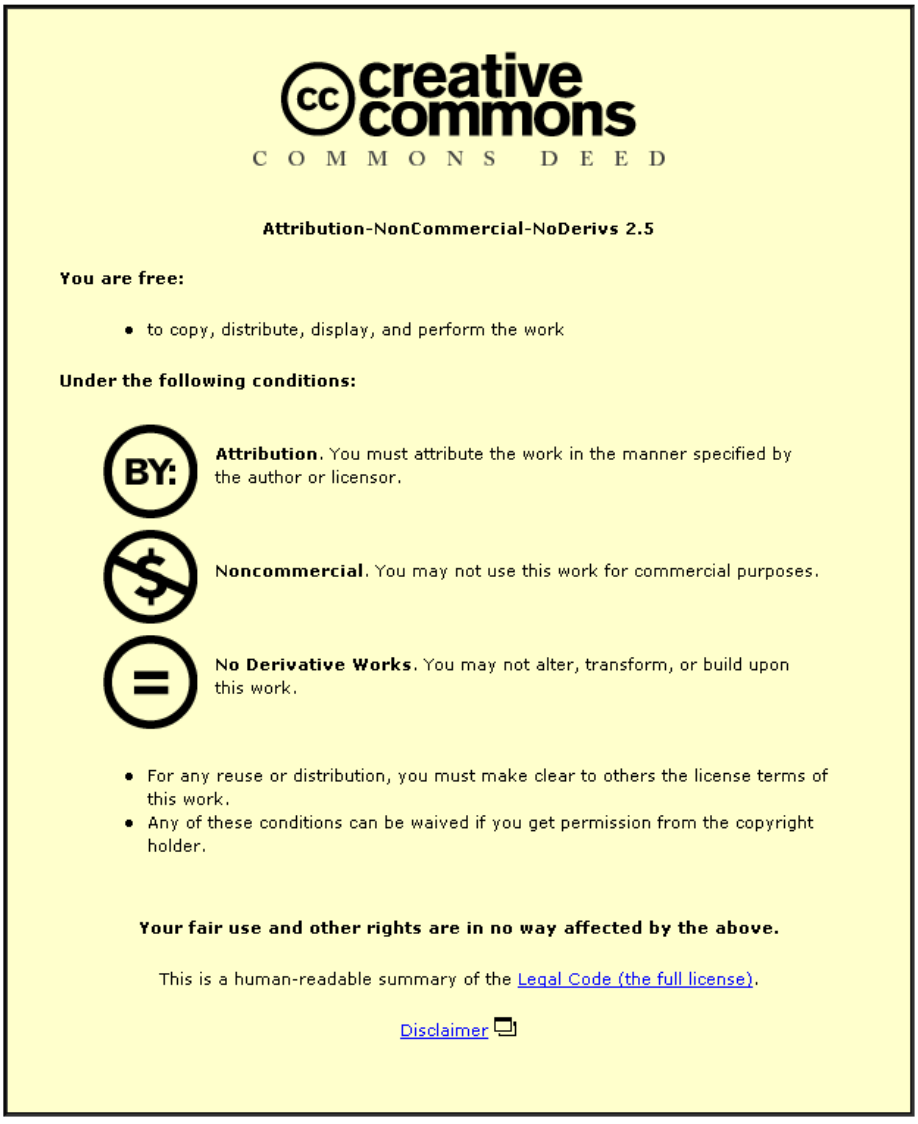

creative commons

COMMONS DEED

Attribution-NonCommercial-NoDerivs 2.5

You are free:

- to copy, distribute, display, and perform the work

Under the following conditions:

Attribution. You must attribute the work in the manner specified by the author or licensor.

Noncommercial. You may not use this work for commercial purposes.

No Derivative Works. You may not alter, transform, or build upon this work.

- For any reuse or distribution, you must make clear to others the license terms of this work.
- Any of these conditions can be waived if you get permission from the copyright holder.

Your fair use and other rights are in no way affected by the above.

This is a human-readable summary of the Legal Code (the full license).

Disclaimer

Equilibrium and dynamic surface properties of trisiloxane aqueous solutions.

Part 1. Experimental results

Hernan A. Ritacco[1], Francisco Ortega[1], Ramon G. Rubio[1],
Natalia Ivanova[2] and Victor M. Starov[2]*

[1] Department of Quimica Fisica I, Faculty Quimica, Universidad Complutense, 28040-Madrid, Spain
[2]Department of Chemical Engineering, Loughborough University, Loughborough, LE11 3TU, UK

*Corresponding author V.M.Starov@lboro.ac.uk

Abstract

Tensiometry, ellipsometry and Brewster angle microscopy were used to measure equilibrium and dynamic surface tension, as well as surface adsorption, of aqueous solutions of trisiloxane surfactants. Complex adsorption curves, including inflection points, have been found for the surfactants with long etoxylated chains. Surface aggregates at the liquid-air interfaces have been detected for the trisiloxanes that show superspreading behaviour onto moderately hydrophobic surfaces, while no aggregates were detected for the shorter trisiloxanes. The latter suggests that those surface aggregates may act as reservoirs of surfactant molecules to maintain the required surface tension in the course of spreading.

1 Introduction

The ability of some siloxane surfactants to promote the rapid spreading of aqueous solutions on moderately hydrophobic surfaces was reported in the 1960s [1-3]. More recently Zhang et al. have reported a similar behaviour in a new family of glucosamide-based surfactants [4]. This so-called superspreading (or superwetting) is of a great interest in different technologies. Examples include the spreading of coatings and inks on plastics and metals, and of pesticides or fertilizers on

hydrophobic leaf surfaces. There is a number of proposed mechanisms of superspreading. We mention below only three of them. (a) According to [5] the spreading coefficient, $S = \gamma_{sv} - (\gamma_{sl} + \gamma)$, remains positive due to the rapid adsorption of surfactant molecules at the air-solution and solid-liquid interfaces as the perimeter of the drop expands. To maintain the surfactant concentration at the contact line (liquid-gas-solid contact line) the flux from bulk to the interfaces (liquid-vapor; solid-liquid) should be faster than the dilation rate of the perimeter [5]. (b) The next mechanism proposed is driven by Marangoni forces (force due to surface tension gradients). Because the apex of the drop is not depleted continuously by adsorption at the solid surface, the surfactant concentration at the apex may be greater, and then its surface tension lower, than at the perimeter [6]. The latter produces a flux that pulls liquid from the apex to the perimeter and is a driving force of the spreading. To maintain the difference in surface tension between the apex and the perimeter, surfactant molecules must adsorb continuously and fast enough to the air-liquid interface. Both mentioned mechanisms are represented in Fig. 1. (c) The next mechanism was suggested in [7] and the assumption made on the consideration of a climbing of relatively thick film of trisiloxane solution against gravity force. The duration of the process was slow enough and substantially bigger than characteristic times of adsorption on both liquid-air and solid liquid surfaces. The latter allowed the authors to suggest that the surface forces action in those films at concentration above CAC is much longer than it is usually assumed [7].

Kumar et al. [8] have carried out dynamic surface tension measurements of trisiloxane solutions in order to check whether the adsorption dynamics fulfilled the conditions imposed by mechanisms (a) and (b). They used the Frumkin equation in combination with direct measurements of the equation of state. They claimed that Frumkin equation fits well their dynamic surface tension data for relatively low concentrations, and reached the conclusion that the diffusion of surfactant monomers cannot provide the necessary amount of surfactants to maintain the spreading rate

measured considering only mechanism (a) or mechanism (b). Note that the dynamic surface tension experiments of Kumar et al. [8] did not cover the short time range $t < 1$ s.

Kumar et al. [8] suggest that bulk aggregates should play an important role in maintaining the necessary surfactant flux to the perimeter of the expanding drop by adsorbing directly onto the interfaces. It have been pointed out [9,10] that non-turbid solutions may behave as superspreaders, which means that bulk aggregates are not strictly necessary. The formation of aggregates in adsorbed monolayers at a liquid-air interface has been reported earlier [11-13] for the case of insoluble or only slightly water soluble surfactants, such as dodecanol, but they have never been reported earlier for soluble trisiloxane surfactants.

Below equilibrium and dynamic surface tension measurements of trisiloxane solutions are presented in the time range down to 1 ms. Brewster angle microscopy and ellipsometry measurements were also carried out both below and above of the critical aggregation concentration (CAC). These experiments point out that *surface* aggregates form even at concentrations below the CAC. These surface aggregates may play a very significant role as reservoirs of surfactant monomers to maintain the necessary surface tension and the surfactant flux for the high rate spreading (superspreading).

2 Materials and Methods

Trisiloxane surfactants used were supplied by Dr Randall Hill, Dow Corning Corporation. The purity of the samples was 99% with a monodispersity of 99%. The trisiloxanes will be identified by the notation TN, where N is the number of [-O-CH_2-CH_2-] groups. Double distilled and deionised water from a milliQ-RG unit has been used in all the experiments. Its resistivity was always higher than 18 M$\Omega \times cm^{-1}$. All aqueous trisiloxane solutions were made in a phosphate buffer (pH=7) in order to avoid hydrolysis. All the solutions were prepared 2 hours before use. The

dynamic surface tension was measured with a combination of the following techniques. A Kruss K10 plate tensiometer with a roughened Pt-plate, and a home-made pendant drop technique with ADSA software have been used for measurements in the long-time regime (t > 5 s). The glass cell used in the plate tensiometer was designed in order to minimize the evaporation; the stability of the height of the liquid-air interface was checked through the reflectivity of a He-Ne laser beam. A Lauda MPT-2 maximum bubble pressure tensiometer was used for measurements in the short-time regime (1ms < t < 1 s). Viscosity corrections were carried out according to Freer et al. [14].

In all experiments the temperature was controlled to within 0.02 degrees by circulating water from a Techne thermostat. A Nanofilm EP-3 image ellipsometer (Germany) was also used in these experiments. A NIMA minitrough was positioned on the goniometer plate, allowing us to measure the surface tension simultaneously with measurement of the ellipsometric angles. A PMMA cover with two holes for the incident and the reflected beams was used in order to minimize the evaporation. The incident laser beam (λ = 532 nm) was focused on a 30×30 μm^2 surface. To improve the sensitivity of the measurement, the experiments were performed at the incident angle of $\theta = 53^{\circ}$, which is close, but slightly above, the Brewster angle for pure water ($\theta = 52^{\circ}$).

From the measurements of the two ellipsometric angles, related to the change in intensity between the incident and the reflected beams, and Δ, related to the phase shift, the thickness of the monolayer was extracted. The precision on the ellipsometric angles is c.a. 0.0006. In order to decrease the uncertainty in the measurements of the thickness and the refractive index of the interface, solutions of trisiloxane in water, D_2O, and mixtures of H_2O and D_2O were measured [15]. In addition Brewster angle photos were taken at selected values of surface pressure Π, where $\Pi = \gamma_0 - \gamma$, where γ_0 and γ the surface tension of pure water and trisiloxane solutions, respectively. The self-diffusion coefficients, *D,* of trisiloxanes were measured in chloroform solutions by pulsed gradient NMR using a Bruker AMX500 apparatus. The values of *D* in water

solutions were calculated using the Stokes-Einstein equation and the viscosities of water and chloroform. The refractive index of pure liquids was measured with a Carl Zeiss refractometer. The differential refractive index for the solutions was measured with a Brookhaven Instruments-DNDC apparatus.

3 Results

3.1 Equilibrium surface tension

Fig. 1 shows the equilibrium isotherms for all the trisiloxanes studied here (n = 4, 5, 6, 7, 8 and 9) at a temperature of 298.15 K. The isotherms were also measured at T = 283.15 K, results not shown (however, see the discussion below). The critical aggregation concentrations (CACs) were obtained from these results and they are summarized in Table 1. For T8 at 298K we obtained a CAC, which is very close to the value obtained by Kumar et al. [8], similar to the values given by Svitova et al. [16] and Ananthapadnabhan et al. [17] for a commercial trisiloxane Silvet 77 (n=7.5). The present results indicate that the CAC slightly increases with the length of the polyether chain, n. The increase of the CAC is expected because of the increase of the hydrophilic tail (ethoxy groups) whilst the hydrophobic head remains the same for all n. A slightly increment of the CAC concentration is also observed when temperature was decreased from T=298.15 to 283.15 K (see Table 1), which is consistent with the fact that the solubility of the ethoxy groups in water decreases as temperature increases.

3.2 Ellipsometry

In Table 2 we present the ellipsometric thickness, d, of the air-solution interface as a function of surfactant concentration for T8 at 298K. Those results were obtained using a single slab model [18]. A two slabs model was also used. In the latter case the refractive index of the upper layer (the polyether chains) was assumed to be that of liquid polyether surfactants, and the refractive index of the second layer (the trisiloxane head) was assumed to be equal to that of poly(methyl siloxane)

[17]. The thickness obtained using the two-slabs model were equal to those of a single layer model within the estimated uncertainty. In order to make a further test of the thickness values we have followed Nylanders method [13] and made ellipsometric measurements for T8 solutions formed in D_2O and mixtures of D_2O and H_2O. The obtained values of d were the same as in pure water within the experimental error. Similar ellipsometric thicknesses were found for T9 and T6.

The surface concentration of surfactants at equilibrium, Γ, can be calculated from the ellipsometric thickness according to the following equation[15]:

$$\Gamma = \frac{n_f - n_0}{dn/dc} d, \qquad (1)$$

where n_0 and n_f are the refractive indexes of the solvent and the pure trisiloxane, respectively; dn/dc is the refractive index increment. The values of n_f for T4 to T9 differ in less than 0.07%, being n_f = 1.4427 for T9 at λ = 532 nm. A similar result was reached for dn/dc, which is the same for all the trisiloxanes investigated, dn/dc = (0.1795 ± 0.0002)×10^{-3} m^3/kg measured at 298.15 K and λ = 532 nm. As an example, Table 2 summarizes the values of Γ obtained for T8 using Eq. (1). The value obtained from the isotherms (Fig. 1) and Gibbs equation: $\Gamma = \frac{1}{RT}\frac{d\gamma}{d(\ln c)}$, is $\Gamma \sim 2\times10^{-6}$ mol/m^2 for concentrations close but below the CAC. Kumar et al. [8] found values of $\Gamma \sim 2.5\times10^{-6}$ mol/m^2 and 1.97×10^{-6} mol/m^2 for T4 and T12, respectively, using the Langmuir equation and $\Gamma \sim 3.2\times10^{-6}$ mol/m^2 and 2.4×10^{-6} mol/m^2 by fitting the isotherms using the Frumkin equation for T4 and T12.

In Fig. 2a we present equilibrium surface tension data for T8 (comparison of our experimental data with those presented in [8]). In Fig. 2b the total surface concentration measured by ellipsomentry is presented. The latter figure shows that the total surfactant concentration (aggregates + single molecules) levels off above CAC.

3.3 Dynamic surface tension

Fig. 3 shows the dynamic surface tension of T4 and T8 at several concentrations below the CAC. Those dependencies are similar for the other trisiloxanes (T5, T6, T7 and T9) at those concentrations.

However, at concentrations close to the CAC and above the dynamic surface tension behaviour at short adsorption times for T6, T7, T8 and T9 behaviour differs from that for T4 and T5: there are inflection points on those dependences of dynamic surface tension at short adsorption time for the case of T6, T7, T8 and T9 and no inflection point for T4 and T5. Fig. 4 shows the behaviour of dynamic surface tension at short adsorption time for T9 solution (inflection points are marked by arrows). Similar dependencies were obtained for T6, T7 and T8 solutions. Difference in their behaviour seems to indicate that, for TN with N> 6, some additional processes are taking place at the surface, as, for example, reorientation, a phase transition or a formation of surface aggregates.

Both Figs. 3a and 3b clearly demonstrate the presence of initial stage (a lag time) during adsorption at liquid air interface. Note that the lag time decreases as the bulk concentration of surfactants increases. A similar lag time was found in the course of spreading trisiloxane solutions over hydrophobic substrates [20-22]. As in the case of adsorption the lag time in this case decreases as the bulk concentration of surfactants increases.

3.4 Surface aggregation at the interface

The previous observation (Fig. 4) could probably mean a surface phase transition or the formation of aggregates at the interface.

In order to check for the presence of aggregates or a 2D phase transition, we have performed BAM measurements for selected values of γ. Fig. 5 shows three pictures for the T-9 solutions at 298 K and for values of γ = 62.5, 45.12 and 24.82 mN/m. For low surfactant concentrations the surface is almost homogeneous (Fig.6a). However, for $c > 10^{-3}$ mol/m^3 some inhomogeneities are clearly

visible, that become more dense as the bulk concentration, *c*, increases to form finally fractal like clusters. The similar aggregate formation at liquid-air interface was detected for T6, T7 and T8 (Fig. 6). No inhomogeneities/aggregates were found for T-4 and T-5, however, because the size resolution of BAM measurements is about 10^{-6} m we cannot claim the absence of aggregates smaller than this limit. At any case this result seems to be in accordance with what we found in the dynamic surface tension measurements (Fig. 4). It is important to emphasise that all samples were prepared just before use in phosphate buffer and, hence, the hydrolysis of the trisiloxanes must be discarded as the source of the surface aggregates. It is the first time that the existence of surface aggregates has been reported at the air-solution interface of trisiloxane solutions. Even though surfactant aggregates have been previously reported by the group of Vollhardt [11-13] there seem to exist some differences with the results reported here for trisiloxanes. In effect, the adsorption γ vs. t curves were found to present a break point associated to the formation of a surface condensed phase, while in the present case either an inflection point (T9) or no singular point (T8) are observed. This might mean that the surface aggregates are more weakly bound in the case of trisiloxanes than for the surfactants studied by Vollhardt's group. This hypothesis might become visible in dilational relaxation experiments, which will be the object of a future work.

5 Conclusion

Tensiometry, ellipsometry and Brewster angle microscopy were used to measure equilibrium and dynamic surface tension and surface adsorption of aqueous solutions of trisiloxanes surfactants. We show that those surfactants, which show superspreading behaviour, form aggregates on liquid-air interfaces. We have found that trisiloxane surfactants form surface aggregates over a certain bulk concentration and for N > 6. The latter means that the surfactant molecules are present at the liquid-vapour interface in two states. We have associated one of the states to surfactant as being adsorbed as a monomer, and the other corresponding to the surfactant adsorption as a part of a surface

aggregate. These surface aggregates could act as reservoirs of surfactant monomers in the course of spreading.

Acknowledgments

The work of R.G. Rubio, F. Ortega and H. Ritacco was supported in part by MEC through grant FIS2009-14008-002-01, and by CAM through project INTERFASES (S-0505/MAT-0227). H Ritacco was supported by MEC under Juan de la Cierva contract. We thank JE-Rubio for the ellipsometry results. V Starov and N Ivanova acknowledge Engineering and Physical Sciences Research Council, UK support (Grant EP/D077869/1). R.G.Rubio and V. Starov acknowledge support by Marie Curie "Multiflow" research project.

References

[1] E.G. Schwarz, W.G. Reid, Ind. Eng. Chem. 56 (1964) 26-35.

[2] D.L. Bailey, I.H. Petersen, W.G. Reid, Chem. Phys. Appl. Surface Active Substances Proc. 4th Int. Congr. 1 (1967) 173-182.

[3] B. Kanner, W.G. Reid, I.H. Petersen, Ind. Eng. Chem. Prod. Res. Dev. 6 (1967), 88-92.

[4] Y. Zhang, G. Zhang, F. Han, Colloids Surf., A: Phys. Chem. Eng. Aspects. 276 (2006**)** 100-.

[5] T.F. Svitova, R.M. Hill, C.J. Radke, Langmuir, 15 (1999) 7392 - 7402.

[6] A.D. Nikolov, D.T. Wasan, A. Chengara, K. Koczo, G.A. Policello, I. Kolossvari. Adv. Colloid Interf. Sci. 96 (2002) 325-338.

[7] N.V. Churaev, N.E. Esipova, R.M. Hill, V.D. Sobolev, V.M. Starov, Z.M. Zorin, Langmuir, 17 (2001) 1338-1348.

[8] N. Kumar, A. Couzis, Ch. Maldarelli, J. Colloid Int. Sci. 267 (2003) 272-285.

[9] M.A. Rosen, L.D. Song, Langmuir, 12 (1996) 4945.

[10] T. Stoebe, Z. Lin, R.M. Hill, M.D. Ward, H.T. Davis, Langmuir, 12 (1996) 337-344.

[11] D. Vollhardt, V.B. Fainerman, G. Emrich, J. Phys. Chem. B 104 (2000) 8536-8543.

[12] V.B. Fainerman, D. Vollhardt, G. Emrich, J. Phys. Chem. B 105 (2001) 4324-4330.

[13] Y.B. Vysotsky, V.S. Bryantsev, V.B. Fainerman, D.Vollhardt, J. Physical Chemistry B. 106 (2002) 11285-11294.

[14] E.M. Freer, H. Wong, C.J. Radke, J. Colloid Inter. Sci. 282 (2005) 128.

[15] J-W. Benjamins, K. Thuresson, T. Nylander, Langmuir, 21(2005) 149.

[16] T.F. Svitova, R.M. Hill, Y. Smirnova, A. Stuermer, G. Yakubov, Langmuir 14 (1998) 5023-5031.

[17] K.P. Ananthapadnabhan, E.D. Doddard, P. Chandar, Colloids Surf. 44(1990) 281-297.

[18] H.G. Tompkins, Users Guide to Ellipsometry; Academic Press, San Diego, 1993

[19] J. Brandrup, E.H. Immergut, E.A. Grulke, Eds., Polymer Handbook, 4th Ed., Wiley Interscience: Hoboken, N.J., 1999.

[20] N. Ivanova, V.M. Starov, D. Johnson, N. Hilal, R. Rubio, Langmuir 25 (2009) 3564-3570.

[21] C.C. Wei Ping, N.A. Ivanova, V.M. Starov, N. Hilal, D. Johnson, Coll. Journal 71 (2009) 1-6.

[22] N. Ivanova, V. Starov, R. Rubio, H. Ritacco, D. Johnson, N. Hilal, Colloids Surf., A: Physchem. Eng. Aspects (2009) doi:10.1016/j.colsurfa.2009.07.030.

Figure legends

Fig. 1. Surface tension isotherms. The lines are fitting curves using the Frumkin isotherm.

Fig. 2. (a) Equilibrium isotherm for T-8. Our experimental points (squares) and Kumar et al.[8] The line is fitted according to Frumkin equation. (b) The surface concentration as a function of concentration. The points are the measured surface concentration data obtained by ellipsometry.

Fig. 3. Dynamic Surface tension (a) T-8, (b) T-4. The lines are fitting curves to guide the eyes.

Fig. 4. Dynamic Surface tension close and above the CAC for T-9 measured with the MBP for short adsorption times.

Fig. 5. BAM images for T9. (a) $c = 1.44\times10^{-4}$ mol/m^3; (b) $c = 3\times10^{-3}$ mol/m^3; (c) $c = 1\times10^{-1}$ mol/m^3.

Fig. 6. BAM images for T6, T7 and T8 at c = 0.002 mol·m^{-3}. The total width of each image represents 400 μm. Inhomogeneities for T6, T7 and T8 at c = 0.002 mol·m^{-3}, i.e. somewhat below the CAC.

Table 1. CACs for all trisiloxane surfactants used here at two temperatures.

Trisiloxane	CAC, mol/m^3	
	T = 283K	T = 298 K
T-4	0.046	0.022
T-5	0.06	0.028
T-6	0.1	0.061
T-7	0.15	0.07
T-8	0.12	0.094
T-9	0.16	0.15

Table 2. Ellipsometric thickness ad surface concentration for T-8 solutions at 298.15 K as a function of concentration. The values of Γ were calculated with Equation (1).

Concentration, mol/m^3	d, nm	$10^7\ \Gamma$, mol/m^2
1.44×10^{-6}	0.2 ± 0.1	1.7 ± 0.3
1.44×10^{-5}	0.3 ± 0.2	2.0 ± 0.3
1.44×10^{-4}	0.4 ± 0.2	4.4 ± 0.3
1.44×10^{-3}	0.9 ± 0.2	8.4 ± 0.3
1.44×10^{-2}	0.9 ± 0.2	8.9 ± 0.2
1.44×10^{-1}	1.0 ± 0.1	9.2 ± 0.2

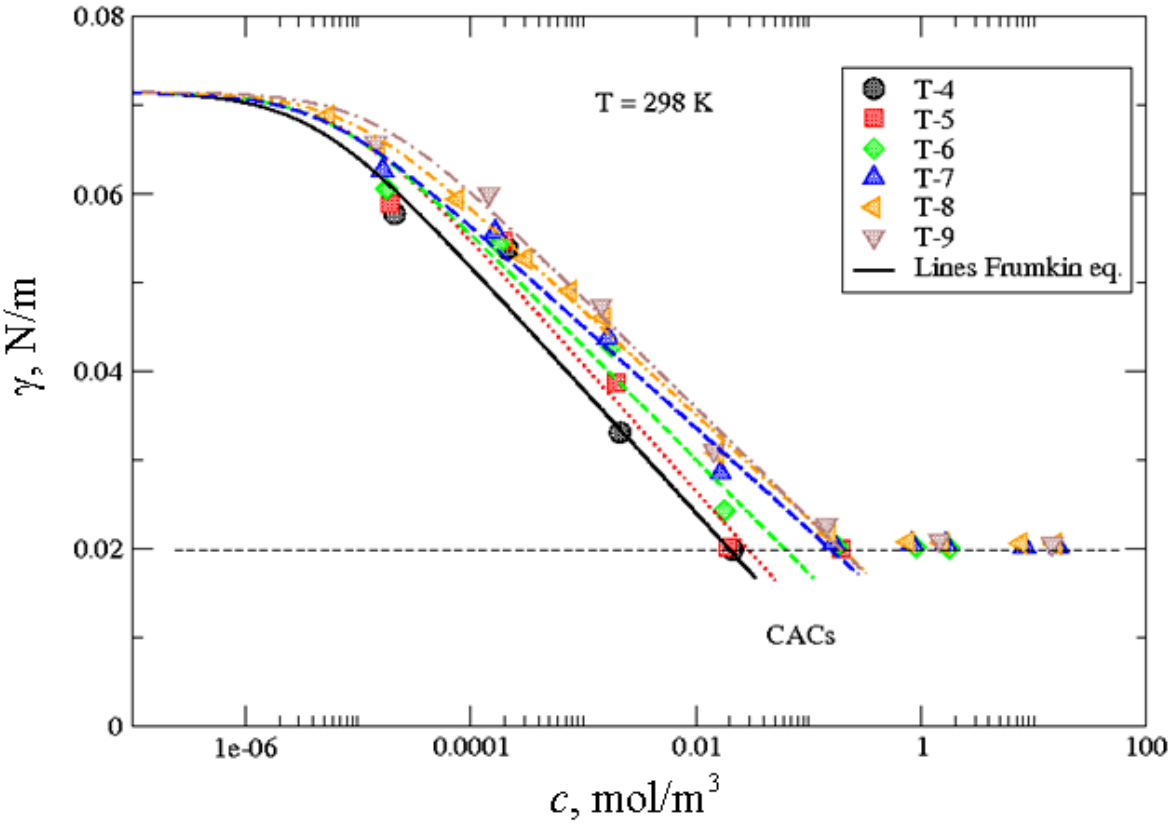

Fig. 1. Surface tension isotherms. The lines are fitting curves using the Frumkin isotherm.

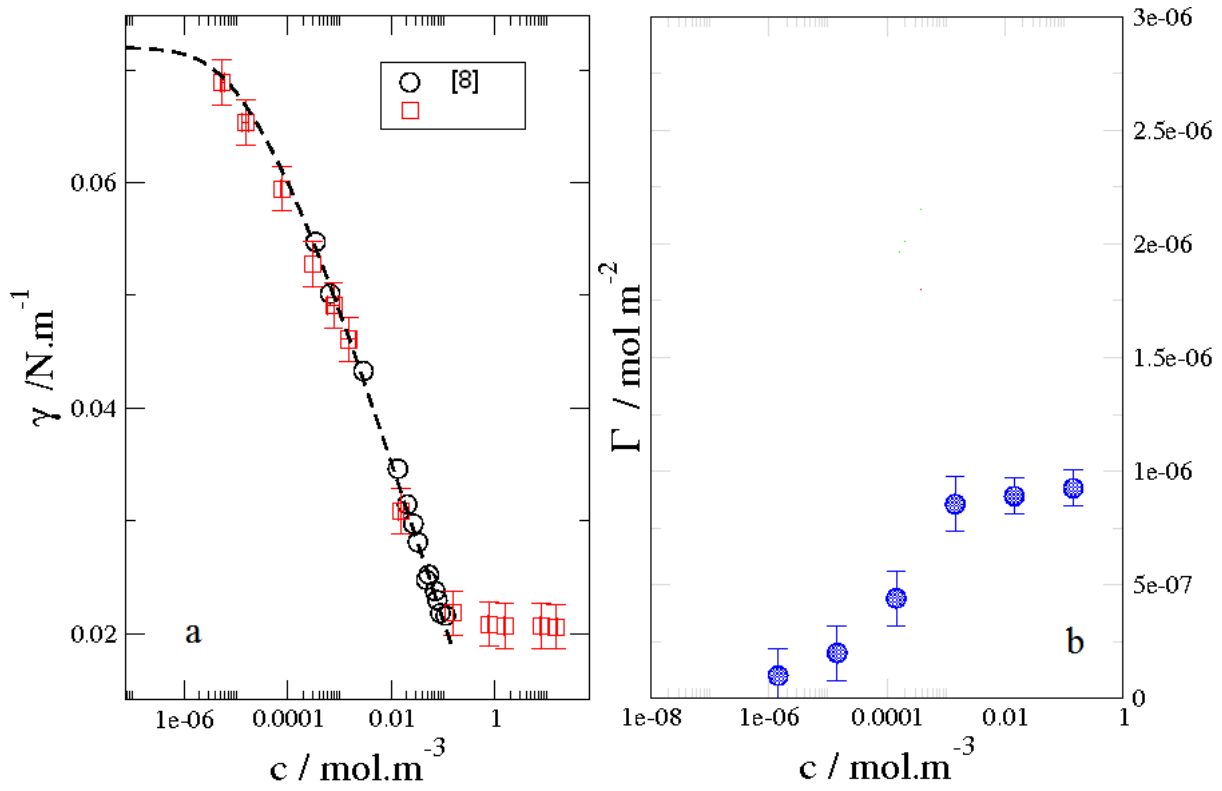

Fig. 2. (a) Equilibrium isotherm for T-8. Our experimental points (squares) and Kumar et al.[8] The line is fitted according to Frumkin equation. (b) The surface concentration as a function of the bulk concentration obtained by ellipsometry.

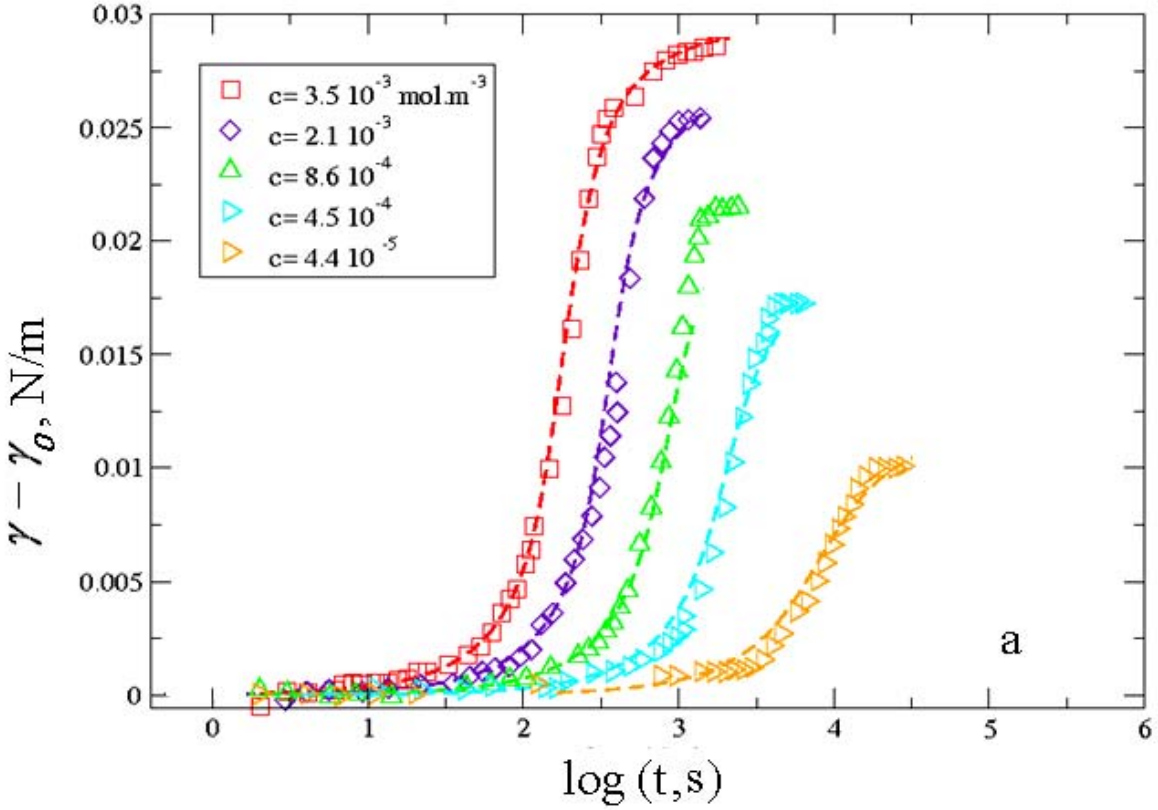

Fig. 3a. Dynamic Surface tension for T-8. The lines are fitting curves to guide the eyes.

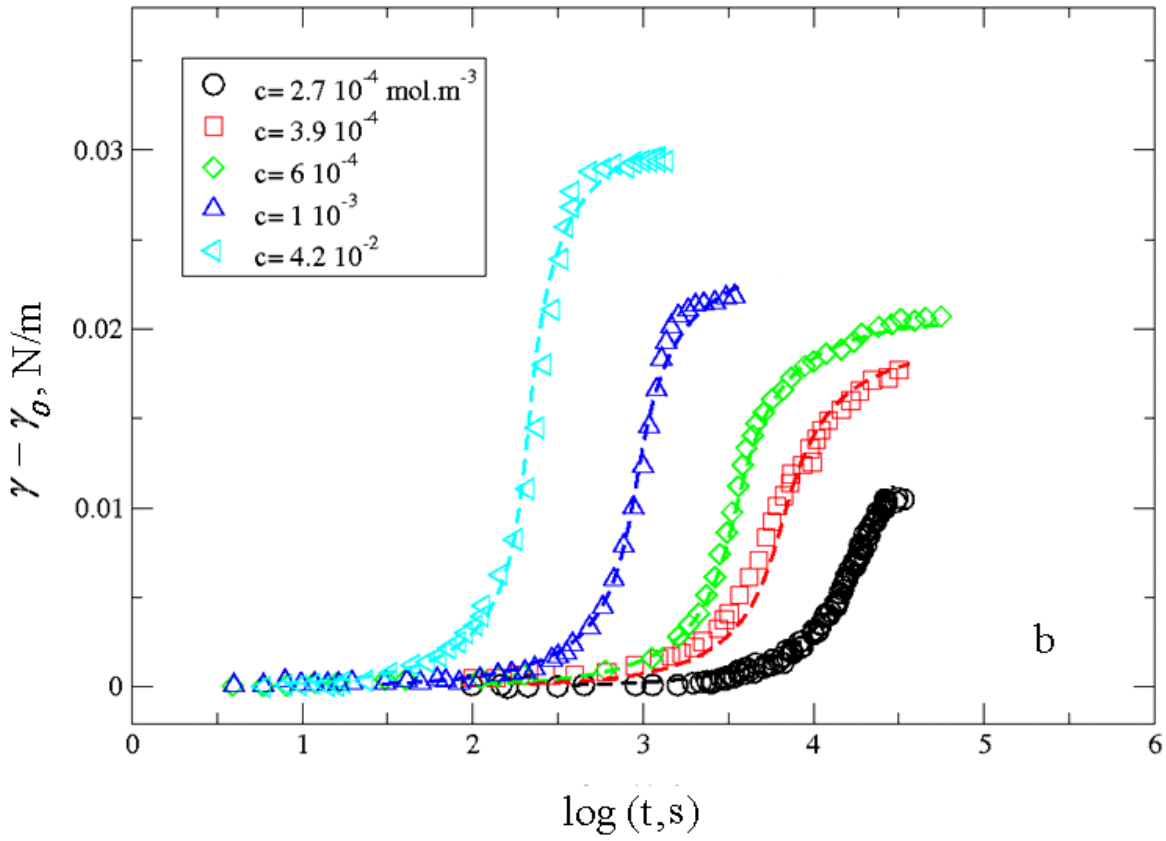

Fig. 3b. Dynamic Surface tension for T-4. The lines are fitting curves to guide the eyes.

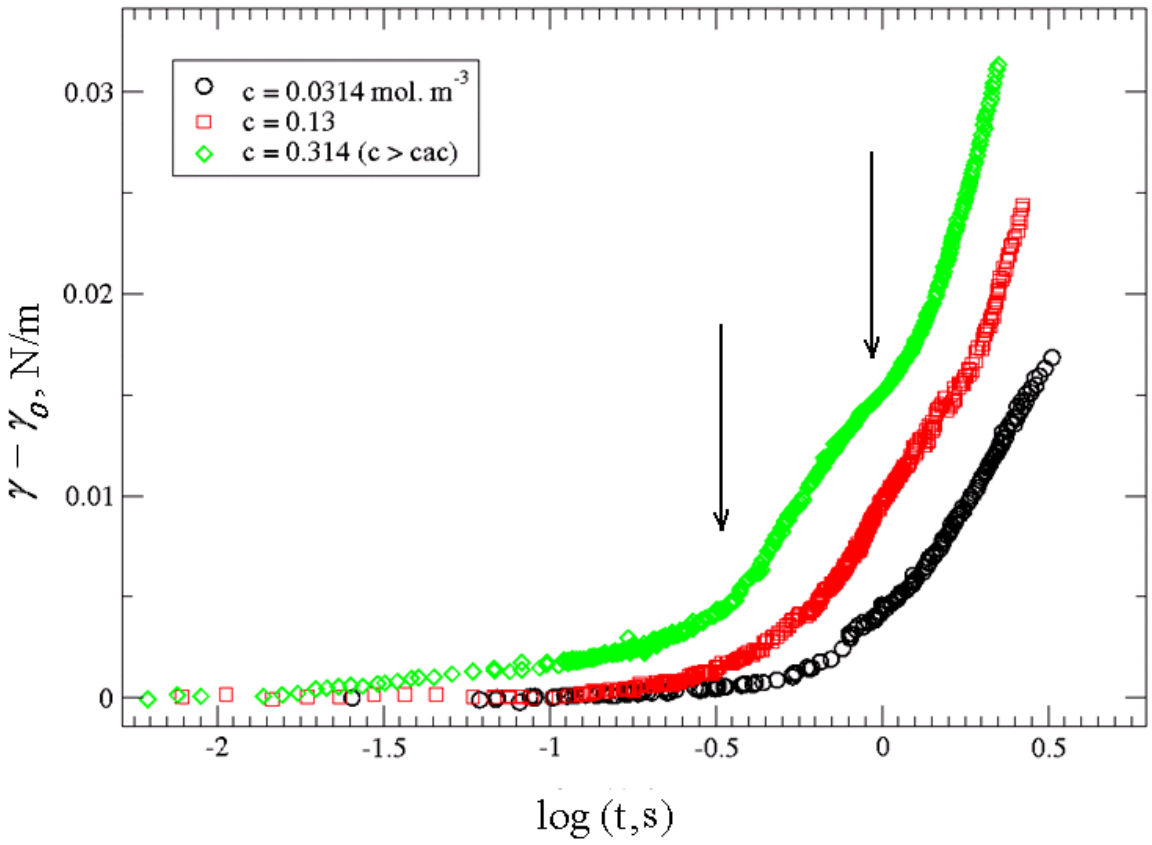

Fig. 4. Dynamic Surface tensions close and above the CAC for T-9 measured with the MBP for short adsorption times.

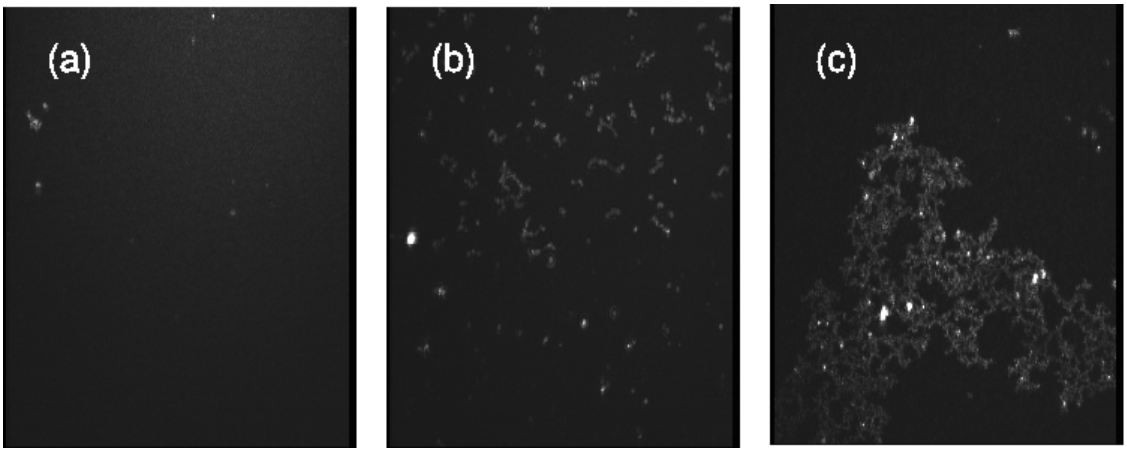

Fig. 5. BAM images for T9. (a) $c = 1.44\times10^{-4}$ mol/m^3; (b) $c = 3\times10^{-3}$ mol/m^3; (c) $c = 1\times10^{-1}$ mol/m^3.

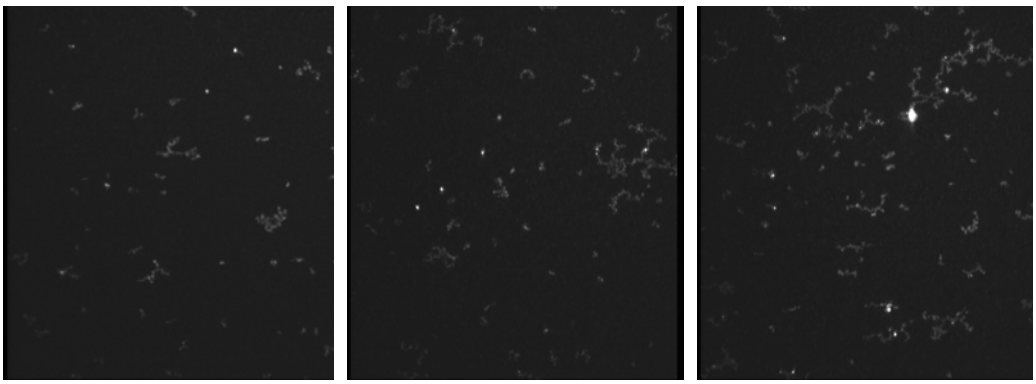

Fig. 6 BAM images for T6, T7 and T8 at c = 0.002 mol·m^{-3}. The total width of each image represents 400 μm. Inhomogeneities for T6, T7 and T8 at c = 0.002 mol·m^{-3}, i.e. somewhat below the CAC.